X-ray and extreme ultraviolet emission induced by variable pulse-width irradiation of Ar and Kr clusters and droplets

E. Parra,[1,*] I. Alexeev,[1] J. Fan,[1] K. Y. Kim,[1] S. J. McNaught,[1,2] and H. M. Milchberg[1]

[1]*Institute for Physical Science and Technology, University of Maryland, College Park, Maryland 20742*

[2]*National Institute of Standards and Technology, Gaithersburg, Maryland 20899*

(Received 13 July 2000)

Measurements are presented of x-ray (>1.5 keV) and extreme ultraviolet (EUV, $\lambda = 2-44$ nm) emission from argon and krypton supersonic gas jets at room ($T = 300$ K) and cryogenic ($T = 173$ K) temperatures irradiated with constant energy (50 mJ), variable width laser pulses ranging from 100 fs to 10 ns. Two regimes of jet operation are explored: cluster formation (radius<100 nm) and droplet formation (radius>1 μm). The results for both clusters and droplets can be understood in terms of two time scales: a short time scale for optimal resonant absorption at the critical density layer in the expanding plasma, and a longer time scale for the plasma to drop below critical density.

PACS number(s): 52.40.Nk, 36.40.Vz

In recent years, the interaction of high intensity laser pulses with atomic clusters has become a very active area of research [1]. The clusters are van der Waals bonded assemblies of $\sim 10^2-10^7$ atoms which form during rapid cooling during flow through a supersonic nozzle [2]. Such short pulse heated clusters eject keV electrons and highly charged ions with kinetic energies up to 1 MeV, generate strong emissions of x rays well into the keV range, and exhibit very high (> 95%) laser energy absorption [1]. Recently, fusion has been demonstrated using collisions of fast ions from heated deuterium cluster explosions [3]. Laser heating of clusters is dominated by collisional absorption, a process more typical of solid targets. This enhances the energy absorbed compared to that in unclustered subcritical density gases and makes laser irradiated cluster gas an efficient source of extreme ultraviolet (EUV) emission for microscopy or lithography [4].

For light source applications, a natural goal is to maximize EUV and x-ray emissions from the cluster jet target for a given laser pulse energy. An intrinsic limitation on laser coupling efficiency is the cluster lifetime, which we define to be the time $\tau_{\rm crit}$ for the heated cluster plasma to expand to an electron density below critical, whereupon laser light absorption will decrease significantly. For pulses longer than this, coupling should be no better than to an unclustered gas of the same average density. This suggests that the EUV/x-ray emissions from laser-heated clusters should be a strong function of pulsewidth.

In this paper we examine x-ray (>1.5 keV) and EUV($\lambda = 2-44$ nm) emissions from laser heated supersonic argon and krypton gas jets at room temperature ($T_0 = 300$ K, ''uncooled'') and at cryogenic temperature ($T_0 = 173$ K, ''cooled''), using laser pulses of constant energy (50 mJ) and variable pulse width in the range 100 fs to 10 ns. The jet is operated in two regimes: cluster generation (uncooled Ar and Kr, and cooled Ar), where the cluster radius is much smaller than a laser wavelength, and a droplet formation regime (cooled Kr), where the droplet radii are comparable to or larger than the laser wavelength. We find that the results for both clusters and droplets can be understood in terms of two time scales: a short time scale for optimal resonant absorption at the critical density layer in the expanding plasma, and a longer time scale for the plasma to drop below critical density.

In our experiment, the supersonic nozzle has a jet throat diameter (d) of 500 μm and an expansion cone half angle (α) of 5°. The valve body is encased in a copper cooling yoke connected to a liquid nitrogen dewar. For the experiments reported here, under cooled operation the valve body was kept at $T_0 = 173$ K, and the pulsed valve was operated at a backing pressure of $P_0 = 500$ psi with a valve opening time of ~ 450 μs. To heat the jet we used a Ti: sapphire chirped pulse amplification laser ($\lambda_0 = 800$ nm, 10 Hz), to which the pulsed valve was synchronized. The pulsewidth variation was achieved by detuning the grating compressor or inserting an adjustable mask in the pulse stretcher. The laser beam was focused ~ 1 mm below the nozzle orifice, 1.3 cm downstream from the nozzle throat, using an $f = 285$ mm MgF_2 lens. The measured 16.6 μm full width at half maximum (FWHM) focal spot corresponds to a peak vacuum intensity of 1.3×10^{17} W/cm^2 for 100 fs pulses. The EUV spectra (2–44 nm) were built up by scanning the exit slit of a 1.5-meter grazing incidence vacuum monochromator equipped with a windowless electron multiplier. The x-rays were measured using a silicon photodiode (IRD, AXUV- 100) with 150 nm aluminum and 25 μm beryllium filters, which strongly attenuated x rays below ~ 1.5 keV. Both the EUV and x-ray instruments viewed the jet perpendicular to the laser propagation axis.

Direct measurement of cluster size is difficult, although rough estimates are possible [1,5]. For large rare gas clusters, the final mean cluster size (atoms per cluster) has been shown to be reasonably well predicted by the expression $\langle N \rangle = 33(\Gamma^*/1000)^{2.35}$ (for $\Gamma^* > 1000$), where Γ^* is the dimensionless ''Hagena parameter'' given by $\Gamma^* = k[d/\tan(\alpha)]^{0.85} P_0 T_0^{-2.29}$ [2,6,7], where $k = 1650$ for Ar and $k = 2890$ for Kr and the other parameters are indicated in

*Email address: riq@wam.umd.edu

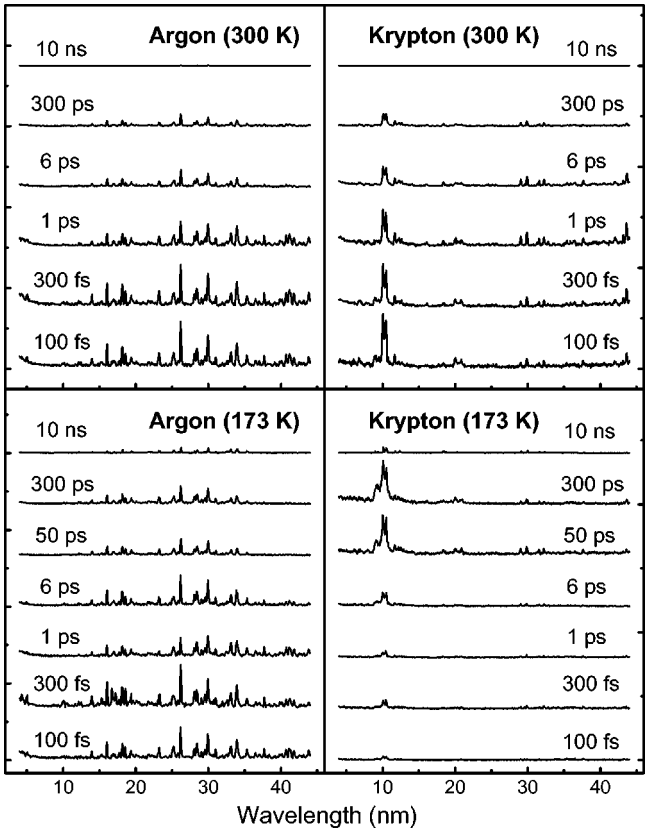

FIG. 1. EUV spectra for argon and krypton for cooled ($T=173$ K) and uncooled ($T=300$ K) jet operation for the full range of laser pulsewidths ($\tau=100$ fs-10 ns).

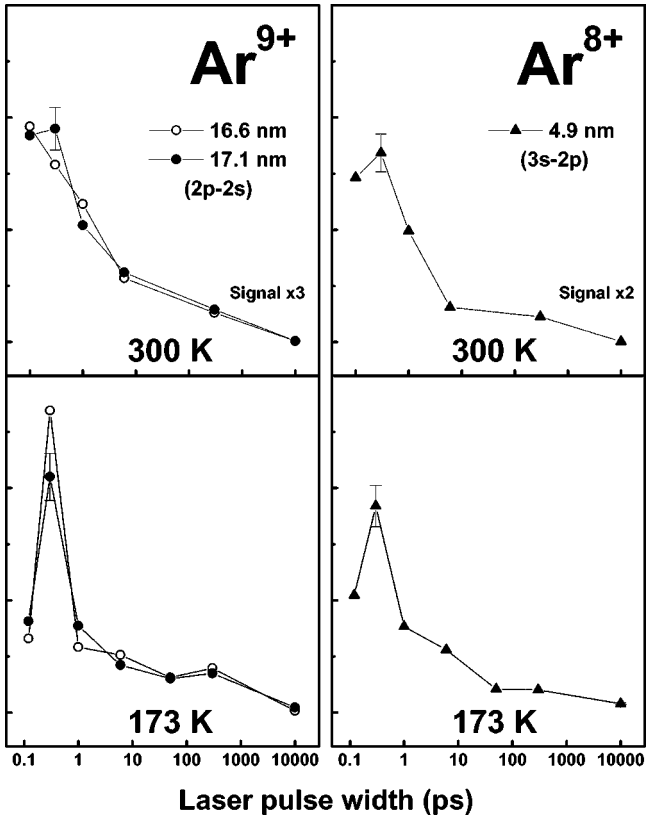

FIG. 2. Time integrated EUV emission from selected *L*-shell $Ar^{9+,8+}$ lines at $T=300$ and 173 K as a function of laser pulse width. The signal scale is linear. Error bars represent maximum shot-to-shot fluctuations.

the nozzle description above. Experiments have shown that for $\Gamma^*>2000$ the condensed fraction in the cluster beam is above 90% [6]. Hagena-based size estimates are in reasonable agreement with other methods such as Rayleigh scattering [8]. Under our conditions, at $T_0=300$ K we obtain $\Gamma^*_{Ar}\sim 2\times 10^5$ and $\Gamma^*_{Kr}\sim 3\times 10^5$, giving for cluster size and radius $\langle N\rangle_{Ar}\sim 7\times 10^6$ ($R_{Ar}\sim 40$ nm) and $\langle N\rangle_{Kr}\sim 3\times 10^7$ ($R_{Kr}\sim 66$ nm). For $T_0=173$ K, $\Gamma^*_{Ar}=7\times 10^5$, giving $\langle N\rangle_{Ar}=1\times 10^8$ ($R_{Ar}\sim 100$ nm). However, for the Kr jet at $P_0=500$ psi and $T_0=173$ K, the Hagena scaling breaks down and does not apply to our nozzle's operation, as will be discussed below.

Figure 1 shows EUV spectra for Ar and Kr for cooled and uncooled jet operation, for the full range of laser pulsewidths. Qualitative inspection indicates that for both cooled and uncooled Ar, and for uncooled Kr, the spectrally integrated emission is maximized for pulsewidths less than ~1 ps, but for cooled Kr the emission has a broad peak in the ~50–300 ps region. A more detailed view of the pulsewidth dependence is obtained by plotting the relative yields of lines from high ion stages. Figures 2 and 3 show plots for several unblended Ar ion lines (*L* shell: Ar^{8+} and Ar^{9+}) and Kr ion lines (*M* shell: Kr^{7+} and Kr^{9+}) for both cooled and uncooled jet operation. We find that for both cooled and uncooled Ar (Fig. 2), peak emission occurs for pulses in the range 100–300 fs, with more prominent peaks in cooled Ar closer to 300 fs. However, there is a markedly different pulsewidth dependence in Kr in the cooled compared to uncooled cases (Fig. 3). For uncooled Kr, the emission peaks at less than ~1 ps (~100 fs for Kr^{9+} and near ~1 ps for Kr^{7+} and lower stages), while for cooled Kr there is a small peak near ~300 fs, and a broad, dominant peak appears in the range ~50–300 ps. Furthermore, the spectral shoulder near 9–10 nm (see the Kr plots in Fig. 1), which is a blend of lines from Kr^{10+} and above [9,10] appears weakly only for <1 ps pulses in the uncooled case, but is much more dominant for 50–300 ps pulses in cooled Kr. As our EUV spectra record emission only to ~250 eV, we also measured x-ray emission above 1.5 keV for the same conditions, shown in Fig. 4. In this range *K*-shell Ar, and *K*-and *L*-shell Kr line transitions will contribute. Here it is seen that peak emission occurs at ~300 fs for both cooled and uncooled Ar and Kr, but there is a secondary broad peak centered at ~100 ps for cooled Kr, which is nearly two orders of magnitude larger than in the uncooled case.

A fundamental difference in cooled Kr jet operation was determined by interferometric studies of the laser-jet interaction [11]. While clear interferograms were obtained for cooled and uncooled Ar and uncooled Kr, they were greatly distorted by speckle for cooled Kr, indicating probe beam scattering from particles of at least wavelength size. Particles of this size range are better described as droplets than clusters. Indeed, for a backing pressure of $P_0=500$ psi and $T_0=173$ K, the Kr behind the valve poppet undergoes a gas-to-liquid phase transition [12]. This effect has been seen previously in cryogenic nozzles when cooling argon below 130 K [13] at high backing pressure. Such condensation cannot be described by Hagena's scaling laws.

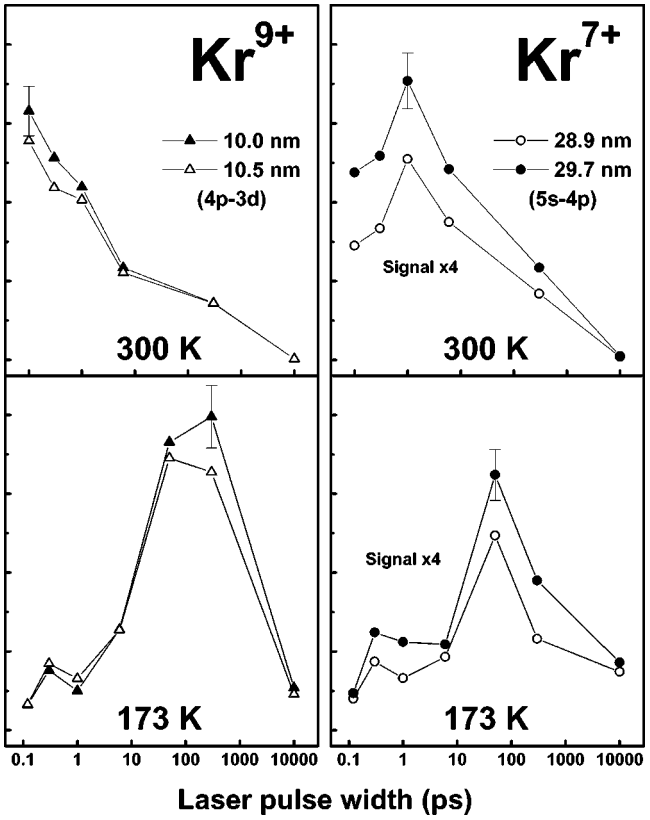

FIG. 3. Time integrated EUV emission from selected *M*-shell $Kr^{9+,7+}$ lines at $T=300$ and 173 K as a function of laser pulse width. The signal scale is linear.

In order to find the droplet sizes, a 1 cm long, 100-μm wide slit was placed centrally below the jet to isolate a thin sheet of droplets. This was backlit with third harmonic pulses (355 nm, 60 ps) from a mode-locked neodymium-doped yttrium aluminum garnet (Nd:YAG) laser system [14]. The light was collected using an $f/2$ lens and relay-imaged to a microscope objective and charge-coupled device (CCD) camera. A histogram of droplet sizes, shown in Fig. 5, was compiled over many shots. The inset to the figure shows a typical low magnification image of the droplet stream. Under these jet conditions, the distribution has a mean droplet diameter of 6.8 μm.

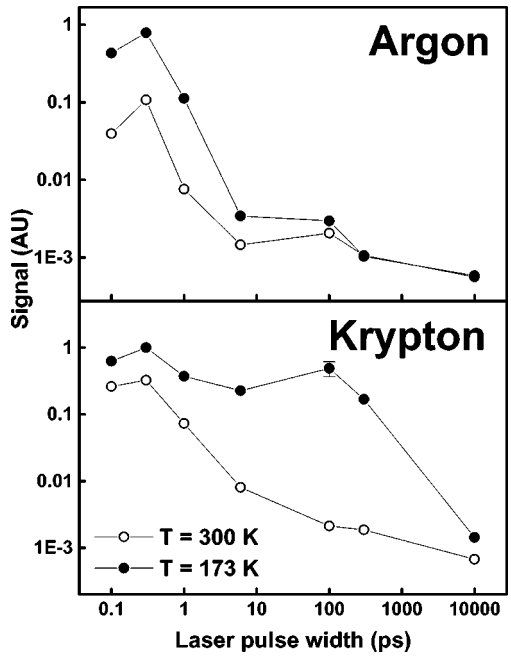

FIG. 4. Argon and krypton x-ray (>1.5 keV) signal at $T=300$ and 173 K as a function of laser pulse width.

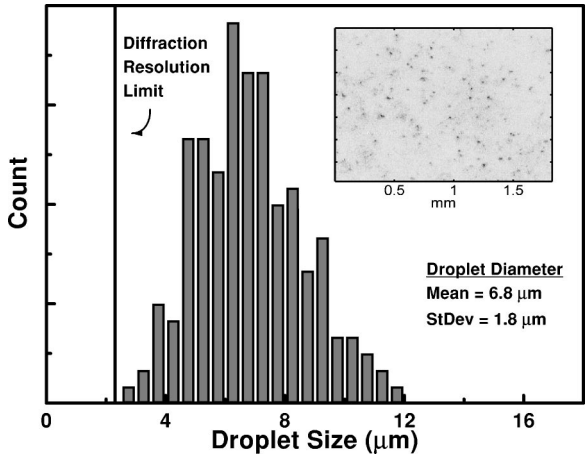

FIG. 5. Histogram of droplet diameters from cooled krypton jet operation ($T=173$ K, backing pressure 500 psi) imaged using 355 nm laser light. The inset shows a typical low magnification image of the droplet stream.

We propose that two time scales govern our results. The first is a longer time scale during which the plasma from an individual cluster or droplet remains above critical density, $\tau_{\rm crit}\sim(N_{e0}/N_{\rm cr})^{1/3}R/c_s$, where R is the cluster radius, c_s is the plasma sound speed, N_{e0} is the pre-expansion electron density of the near-solid density cluster plasma, and $N_{\rm cr}=m\omega^2/4\pi e^2$ is the critical density. For $\lambda=800$ nm, $N_{e0}\sim 2\times10^{23}\,{\rm cm}^{-3}$, $R_{\rm Ar}\sim 40$ nm and $R_{\rm Kr}\sim 70$ nm (from discussion above), and estimating $c_s\sim 2\times10^7$ cm/s for plasma temperatures of at least several hundred eV, we get $\tau_{\rm crit}^{\rm Ar}\sim 1.0$ ps and $\tau_{\rm crit}^{\rm Kr}\sim 1.7$ ps. This is consistent with the emission fall off times in both EUV and x-rays in Ar (both cooled and uncooled) and uncooled Kr, but is at variance with the very long fall-off times for the EUV and x-ray emission in cooled Kr. In that case, simply applying the $\tau_{\rm crit}$ criterion to a droplet radius of $R\sim 3.4\,\mu$m, for all other parameters the same, gives $\tau_{\rm crit}\sim 80$ ps. Since the expansion of a laser-heated droplet is ablative, this timescale is an underestimate, and it may be several times larger. Indeed, our calculations for micron-sized droplets indicate that this is the case [15]. At this point we conjecture that the high efficiency EUV generation seen by other researchers in 10-ns pulse irradiation of cooled Xe gas jets [4], which might at first be taken to be an anomaly considering that $\tau_{\rm crit}$ is a few ps for clusters, is a result of formation of large droplets rather than clusters. In fact, at the backing pressures (200 psi) quoted in [4] Xe can transition into the liquid phase below 230 K [12].

The second, shorter, time scale relates to the finite time for establishing an optimal critical density layer on the periphery of the expanding cluster or droplet plasma in order to maximize resonance absorption [15,16]. We note that >1.5 keV x-ray emission has a peak centered at ~300 fs for *all* cases of Ar and Kr (Fig. 4). Also, the ~300 fs x-ray peak in cooled Kr is larger than the peak at ~100 ps, which is op-

posite to the corresponding EUV results (Fig. 3). This suggests that the EUV peak at ~100 ps represents maximization of the bulk *thermal* heating, while the x-ray peak at ~300 fs represents maximum hot electron generation, which would be consistent with optimal resonant absorption. For linear polarization, an optimal scale length for resonant absorption in the cluster or droplet can be estimated using the plane target result for *p*-polarized electromagnetic waves [16] $|(dN_e/dr)^{-1}N_e| = L_{\mathrm{opt}} \sim 3\sqrt{3}/(8k\cos^3\theta)$, where k is the laser vacuum wave number, θ is the angle between the laser polarization and the local surface normal, and L_{opt} represents a balance between the field's penetration to the critical density surface and its projection along the density gradient. While this expression is more appropriate for the case of droplets ($kR \gg 1$) than the near-field case of clusters ($kR \ll 1$), it gives reasonable results in the near-field regime for $k = \omega_p/c$ and $\theta = 0$ [15]. If we set $L_{\mathrm{opt}} \sim c_s \tau_{\mathrm{res}}$, and use $c_s \sim 2\times 10^7$ cm/s, $\lambda = 800$ nm, and $\theta \sim 0$ (for short scale lengths, resonance absorption is maximized at near-oblique incidence [17], here near the poles of the plasma sphere), we get $\tau_{\mathrm{res}} \sim 400$ fs, in reasonable agreement with the data. As the plasma expands beyond L_{opt} (for $t > \tau_{\mathrm{res}}$), the local heating drops as less laser field penetrates to the critical density surface, and then drops even further for $t > \tau_{\mathrm{crit}}$. However, for droplets τ_{crit} is much larger than for clusters, so that even for $t > \tau_{\mathrm{res}}$, the laser-heating rate integrated over time and droplet volume results in secondary, very wide emission peaks which only fall off beyond ~300 ps. A question remains as to whether there is a difference in the nature of the short time scale coupling mechanism for our clusters and droplets. Although further experiments are needed to answer this question conclusively, our results suggest that the basic mechanism is the same.

The authors thank T. Lucatorto, C. Tarrio, and G. Kubiak for useful discussions. This work is supported by the NSF (Grant No. ECS96-12204).

[1] T. Ditmire *et al.*, Phys. Rev. A **53**, 3379 (1996); Y.L. Shao *et al.*, Phys. Rev. Lett. **77**, 3343 (1996); T. Ditmire *et al.*, Phys. Rev. Lett. **78**, 2732 (1997); M. Lezius *et al.*, J. Phys. B **30**, L251 (1997); M. Lezius *et al.*, Phys. Rev. Lett. **80**, 261 (1998); A. McPherson *et al.*, *ibid.* **72**, 1810 (1994); A. McPherson *et al.*, Nature (London) **370**, 631 (1994); T. Ditmire *et al.*, Appl. Phys. Lett. **71**, 166 (1997); S. Dobosz *et al.*, Phys. Rev. A **56**, R2526 (1997); T. Ditmire *et al.*, Phys. Rev. Lett. **78**, 3121 (1997).

[2] O.F. Hagena and W. Obert, J. Chem. Phys. **56**, 1793 (1972).

[3] T. Ditmire, J. Zweiback, V.P. Yanovsky, T.E. Cowan, G. Hays, and K.B. Wharton, Nature (London) **398**, 489 (1999).

[4] G.D. Kubiak, L.J. Bernardez, K.D. Krenz, D.J. O'Connell, R. Gutowski, and A.M.M. Todd, in *OSA Trends in Optics and Photonics Vol. 4*, edited by G.D. Kubiak and D.R. Kania (Optical Society of America, Washington, DC, 1996), pp. 66–71.

[5] O. Abraham, S. Kim, and G.D. Stein, J. Chem. Phys. **75**, 402 (1981).

[6] J. Wörmer, V. Guzielski, J. Stapelfeldt, and T. Möller, Chem. Phys. Lett. **159**, 321 (1989).

[7] J. Farges, M.F. de Feraudy, B. Raoult, and G. Torchet, J. Chem. Phys. **84**, 3491 (1986).

[8] J.S. Zweiback, Ph.D. thesis, University of California, 1999 (UCRL Report No. LR-134008).

[9] R.L. Kelly, J. Phys. Chem. Ref. Data Suppl. **16**, 1 (1987).

[10] T. Shirai, K. Okazaki, and J. Sugar, J. Phys. Chem. Ref. Data **24**, No. 4, 1577 (1995).

[11] E. Parra and H.M. Milchberg (unpublished).

[12] A.C. Hollis Hallett, in *Argon, Helium and the Rare Gases*, edited by G.A. Cook (Interscience Publishers, New York, 1961), pp. 322–335.

[13] R.A. Smith, T. Ditmire, and J.W.G. Tish, Rev. Sci. Instrum. **69**, 3798 (1998).

[14] T.R. Clark, Ph.D. thesis, University of Maryland, 1998 (unpublished).

[15] H.M. Milchberg and E. Parra (unpublished).

[16] V.L. Ginzburg, *Propagation of Electromagnetic Waves in Plasmas* (Pergamon, New York, 1970).

[17] H.M. Milchberg and R.R. Freeman, J. Opt. Soc. Am. B **6**, 1351 (1989).